# RSC Advances

This is an *Accepted Manuscript*, which has been through the Royal Society of Chemistry peer review process and has been accepted for publication.

Accepted Manuscripts are published online shortly after acceptance, before technical editing, formatting and proof reading. Using this free service, authors can make their results available to the community, in citable form, before we publish the edited article. This *Accepted Manuscript* will be replaced by the edited, formatted and paginated article as soon as this is available.

You can find more information about *Accepted Manuscripts* in the **Information for Authors**.
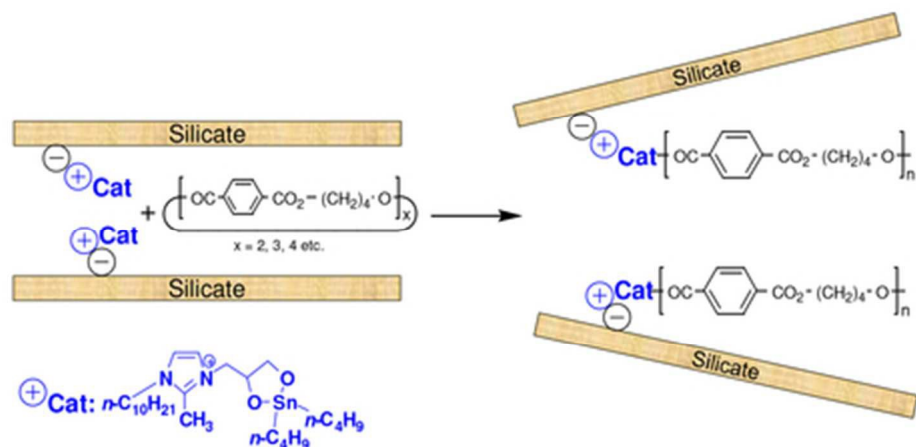
A novel alkylimidazolium salt bearing a 2,2-di-*n*-butyl[1,3,2]dioxastannolane moiety was supported on montmorillonite and used as an effective transesterification catalyst in the entropically-driven ring-opening polymerization (ED-ROP) of macrocyclic oligomers of butylene terephthalate to prepare PBT-clay nanocomposites.
39x19mm (300 x 300 DPI)

Journal Name

ARTICLE

A Novel Tin-based Imidazolium-modified Montmorillonite Catalyst for the Preparation of Poly(butylene terephthalate)-based Nanocomposites Using *in situ* Entropically-driven Ring-opening Polymerization

Lucia Conzatti,[a]* Roberto Utzeri,[a] Philip Hodge,[b] Paola Stagnaro[a]

A novel alkylimidazolium salt incorporating a 2,2-di-*n*-butyl[1,3,2]dioxastannolane moiety was synthesized and characterized. Its effectiveness as a transesterification catalyst in the entropically-driven ring-opening polymerization (ED-ROP) of macrocyclic oligomers of butylene terephthalate (BT-MCOs) was comparable to that of other tin-based transesterification catalysts. A supported version of the catalyst was prepared by ion exchange with the sodium cations present in montmorillonite. X-Ray analysis indicated the imidazolium species entered the galleries between the silicate layers. The supported catalyst was significantly more thermally stable than the non-supported catalyst. Poly(butylene terephthalate)-clay nanocomposites were obtained by the *in situ* ED-ROP of BT-MCOs intercalated between the clay layers, catalyzed by either the supported tin-based catalyst or by a catalyst prepared *in situ* from a supported imidazolium salt with diol moieties and di-*n*-butyldimethoxytin. X-Ray diffraction and transmission electron microscopy indicated that the ensuing nanocomposites exhibit a mix of intercalated and exfoliated silicate nanolayers.

Introduction

Polymer-clay nanocomposites have been studied extensively since the early 1990s.[1-7] Clays are layered silicates and if the clay particles can be exfoliated to give dispersed sheets of silicate, of nano-sized thickness and high aspect ratio, in a polymer matrix, the nanocomposite obtained is expected to have significantly improved thermal and mechanical properties relative to the pure polymer.[2] Usually the polymer is hydrophobic and to improve its compatibility with the hydrophilic clay the alkali metal cations present in the galleries of the clay are ion exchanged with hydrophobic organic cations. The latter are usually tetrasubstituted ammonium cations bearing long alkyl chains. In this way, the silicate galleries not only become more hydrophobic, but at the same time the sheets of silicate move further apart so facilitating the eventual intercalation of the polymer chains.[2]

This paper is concerned with the synthesis of poly(butylene terephthalate) (**1**, **PBT**) – montmorillonite (**PBT-MMT**) nanocomposites prepared using the entropically-driven ring-opening polymerization (ED-ROP) of macrocyclic oligomers (MCOs) of butylene terephthalate (**2**, **BT-MCOs**) (see Fig. 1) with a tin-based transesterification catalyst anchored in the

galleries. The **BT-MCOs** must then enter the galleries to access the catalyst. This maximizes the extent to which polymer is formed inside the galleries, so maximizing exfoliation and the dispersion of the silicate sheets.
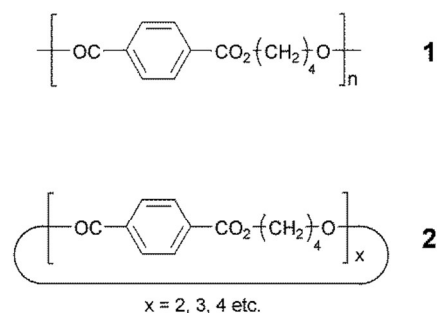

Fig. 1 Chemical structures of **PBT** (**1**) and **BT-MCOs** (**2**).

ED-ROP is a relatively new approach to the synthesis of condensation polymers.[8-13] ED-ROPs used for polyester synthesis are usually based on ring:chain equilibria (RCE), i.e. the well-known equilibria that can exist, under appropriate

reaction conditions, between a polyester and the corresponding family of MCOs: see Scheme 1.[9-10]

The position of the RCE is very dependent on the concentration of the reactants and if MCOs are taken at high concentration and the RCE established, polymer is formed in high yield. It should be noted that at equilibrium *ca.* 1 – 2 % of MCOs remain. ED-ROPs are particularly appropriate for forming the polymer matrix part of the nanocomposite for several reasons. Thus, (i) the ED-ROP takes place without the evolution of volatiles (or indeed any small molecules) that might lead to voids in the matrix; (ii) the MCOs automatically have the correct stoichiometry to form high molecular weight polymer; (iii) ED-ROP can take place very rapidly, so allowing short reaction times; (iv) the MCOs are relatively small and have a relatively low melt viscosity so making it easier for them to penetrate the galleries of the clay than a preformed polymer could.
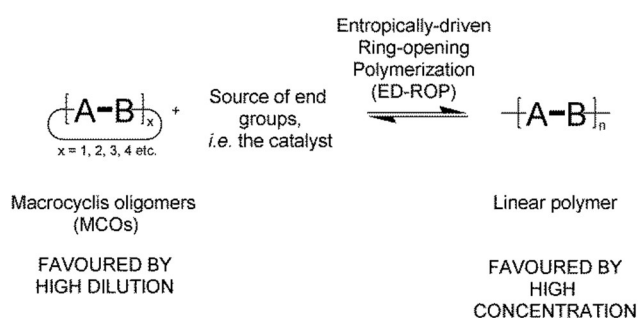
Scheme 1 A generalized ring:chain equilibrium (RCE).

Several approaches have been used to prepare poly(ethylene terephthalate) (PET), poly(trimethylene terephthalate) (PTT) or **1** (**PBT**) – clay nanocomposites.[3-7, 14-17] Some preparations have directly mixed the molten polymers and the clay,[3,4] whilst other composites have been prepared from solutions of the polymer and the clay.[5] In another approach PET-clay nanocomposites were prepared by polymerizing bis(2-hydroxyethyl terephthalate) using either an antimony-based catalyst,[6] or an extra monomer unit tethered in the galleries of the clay.[7] However, a more promising approach is to carry out an ED-ROP of the appropriate MCOs in the presence of the clay.[14-17] Generally the MCOs, clay and a catalyst, most frequently a tin-based catalyst, are carefully mixed and then heated together to bring about the polymerization. These approaches have been shown to lead to nanocomposites with enhanced physical properties. PBT-based nanocomposites containing graphene or graphite oxide were also prepared by *in situ* ED-ROPs.[18,19]

All the above methods required the addition of a transesterification catalyst, usually a tin compound, to the mixture of clay and MCOs. As noted above, ammonium-based compensating cations bearing long alkyl chains are usually employed to increase the compatibility between the clay and polymer matrix. Unfortunately, even under non-oxidative conditions, these organic modifiers begin to decompose at temperatures near 180 °C.[20] This is a problem because higher temperatures than this are needed to achieve the ED-ROPs. Accordingly it is necessary to use more thermally stable 'onium species such as phosphonium,[21-23] pyridinium,[21,23] or imidazolium cations.[3,21-24] In the present project an alkylimidazolium salt bearing a tin-based moiety was used. Since no solvent was used and the percentage of clay is only 3% by weight, only a small fraction of the **BT-MCOs** will be in the clay galleries at any one time. However, the modified imidazolium salt anchored in the galleries acts as an ED-ROP catalyst for the MCOs; the polymer so formed will grow out of the clay to be replaced by more MCOs, as shown in Fig. 2.
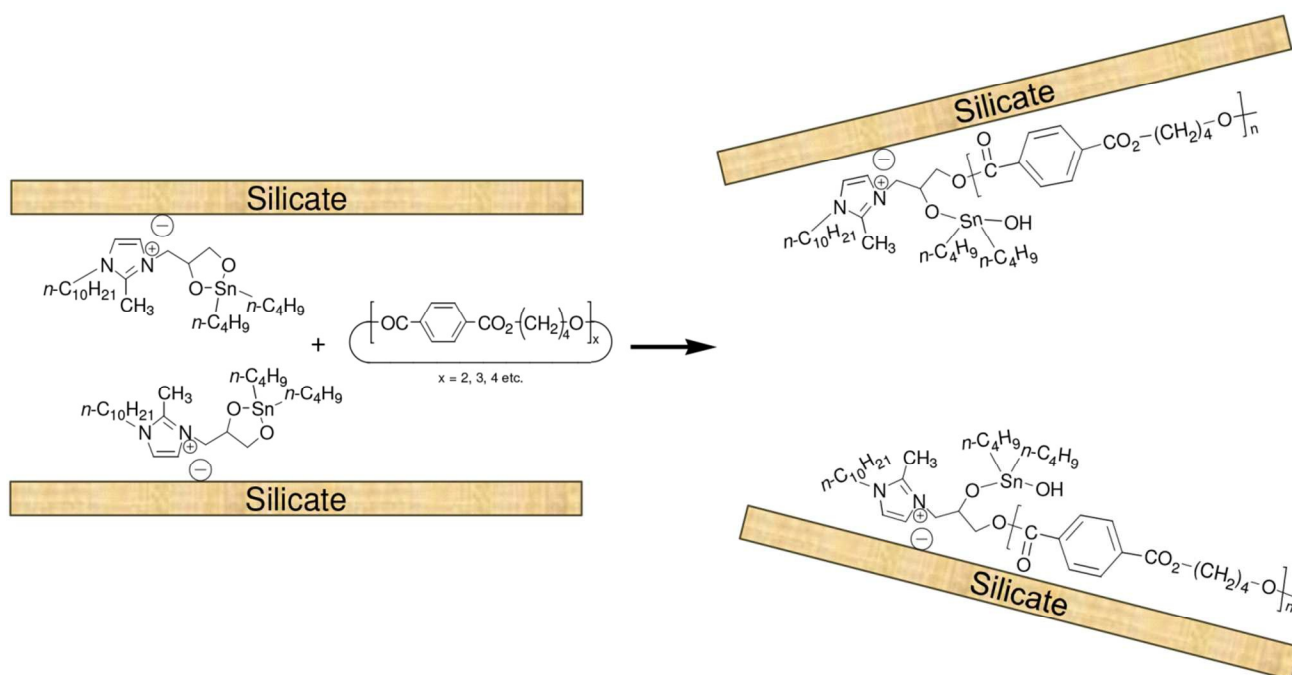

Fig. 2 Schematic depiction of ED-ROP of **BT-MCOs** in between clay layers. .

Experimental

Materials

1-Decyl-2-methylimidazole (**3**), 3-bromo-1,2-propanol (**4**), di-*n*-butyldimethoxytin and analytical grade chloroform, toluene, ethanol and acetonitrile were all obtained from Aldrich and used as received.

Montmorillonite (**MMT**) was DELLITE™ HPS, obtained from Laviosa Chimica Mineraria SpA. By elemental analysis it had 1.55 % sodium, corresponding to 0.67 mmol g^{-1}.

Macrocyclic oligomers of butylene terephthalate (**2**) (**BT-MCOs**) were prepared by cyclo-depolymerization of poly(butylene terephthalate) (**1**) as described previously[12,25] The initial "crude" product had: C, 64.9; H, 5.3; Sn, 0.55%. Expected for $(C_{12}H_{12}O_4)_n$: C, 65.5; H, 5.5; Sn, 0%. The product was dissolved in a minimum amount of chloroform and loaded onto a column of activated basic alumina. The MCOs were eluted using a mixture of chloroform and acetone (94/6 v/v). Evaporation of the eluate to dryness left the "pure" product as a white powder. It had: C, 65.4; H, 5.5; Sn, < 0.1%.

Synthesis of imidazolium salts

The functionalized imidazolium salts **5** and **6** were prepared using the reactions shown in Scheme 2.

3-Decyl-1-(2,3-dihydroxypropyl)-2-methylimidazolium bromide (5). This was prepared using a modification of a literature procedure.[26,27] Thus, under a nitrogen atmosphere a solution of 1-decyl-2-methylimidazole (**3**) in chloroform (9.5 mmol in 31.7 mL) was placed in a two-necked round-bottom flask (100 mL) equipped with a reflux condenser and magnetic stirrer. An excess of 3-bromo-1,2-propanediol (**4**) (10 mmol) was added dropwise over 24 h whilst the mixture was stirred continuously and heated under reflux. The progress of the reaction was monitored by taking samples every 2 h, evaporating off the solvent and volatiles, then measuring the ^{1}H NMR spectrum of the residue: see Electronic Supplementary Information (ESI) for details. When the reaction was complete, removal of the solvent and volatiles under vacuum gave **5** as a pale yellow oil (9.3 mmol, 98%). The reaction was repeated under the same conditions but by using a slight larger excess of **3** and a reaction time of 4 h gaving **5** (9.4 mmol, 99%). The FTIR and ^{1}H NMR spectra are summarized in Table 1.

3-Decyl-1-(2,2-dibutyl[1,3,2]dioxastannolane-4-methyl)-2-metthylimidazolium bromide (6). This was prepared using a modification of literature procedures used to prepare 1,3-dioxa-2-stannanes.[28-31] Thus, an excess of **5** (1.69 mL, 5.3 mmol) and *n*-Bu$_2$Sn(OMe)$_2$ (1.15 mL, 5.03 mmol) were reacted together in toluene (15.3 mL) heated under reflux. The methanol that formed was removed over 2 h by azeotropic distillation using a Dean-Stark apparatus. During this period toluene was added dropwise to the reaction mixture to maintain the volume. Finally the toluene solution was concentrated under vacuum. This left **6** as a viscous oil (5.1 mmol, 97%). The FTIR and ^{1}H NMR spectra are summarized in Table 1.

ED-ROPs of BT-MCOs using no catalyst or non-supported catalysts

The polymerizations investigated are summarized in Table 2. They were carried out in parallel on a 100-mg scale by heating at 190°C for 2 h a series of small vials containing **2** and any other required reactant(s) under a nitrogen atmosphere. The vials were loaded into an aluminium multiple sample holder (fabricated in house) that fitted snugly into a glass Büchi oven.[24] In all cases at the end of the reaction period the product was dissolved in a mixture of methylene dichloride and trifluoroacetic acid (80/20 v/v) then precipitated into methanol. The precipitate was collected, washed three times with methanol, then dried at 65°C under vacuum. The samples were stored in a desiccator. Molecular and thermal characterization was carried out as appropriate using gel permeation chromatography (GPC), differential scanning calorimetry (DSC), and thermogravimetric analysis (TGA).

Preparation of imidazolium-modified clays

Modified clays containing imidazolium salts **5** and **6** were separately prepared by a standard cation exchange technique. The appropriate imidazolium salts (1.5 eq of **MMT** for **5**, 1.1 eq of **MMT** for **6**) were dissolved in ethanol at 50°C for **5** or acetonitrile at 50°C for **6**. In each case the mixture was stirred for 15 min and then added to a vigorously stirred 10% w/v pre-dispersed aqueous suspension of **MMT** at 60°C for 2 h. The final mixture was stirred overnight at 60°C. The imidazolium-modified MMT was collected by filtration, washed several times with a 50/50 mixture of hot solvent/deionized water and further with hot solvent (ethanol or acetonitrile as appropriate). The washing was continued until the filtrate showed the absence of bromide ions on testing with aqueous silver nitrate (0.1 N). The resulting MMTs, designated as **5-MMT** and **6-MMT**, were dried at 65°C under vacuum for 48 h, reduced to fine powders and characterized by X-ray diffraction and TGA. By elemental analysis **5-MMT** had: N, 1.9% corresponding to 0.68 mmol g^{-1} of imidazolium residues per g. **6-MMT** had: N, 1.2; Sn, 2.4%. These correspond to 0.43 mmol of imidazolium residues **3** per g and 0.20 mmol of tin-containing residues per g.

Preparation of PBT-based nanocomposites by ED-ROP

PBT nanocomposites with 3 wt% clay content were prepared by *in situ* intercalative ED-ROP of **2**. Suspensions of the different MMTs (15 mg in 1 mL CH$_2$Cl$_2$) and **2** (500 mg in 8.3 mL CH$_2$Cl$_2$) were separately stirred for 3 h. The suspensions of clay and purified MCOs were then mixed together and stirring was continued overnight. When necessary, Bu$_2$Sn(OMe)$_2$ (1 mol%) was added to the suspensions. The solvent was evaporated off under vacuum and the residues subjected to ED-ROPs. The polymerizations and the reaction work ups were the same as described for ED-ROPs carried out in the absence of **MMT**.

An ED-ROP was also carried out using 2.0 g of purified **2** and **6-MMT** (97/7 wt/wt mixture) in a reaction vessel equipped with a mechanical stirrer. The reaction was carried out under a nitrogen atmosphere at 190°C and for a reaction time of 30 min.

Molecular, thermal, structural and morphological characterization of the produced composites were carried out by GPC, DSC, TGA, X-ray and TEM.

Instrumentation and characterization techniques

Except where indicated otherwise the instruments used in this work were the same as those reported previously.[11-13]

GPC were performed in a mixture of $CHCl_3/CH_2Cl_2/HFIP$ (60/30/10 v/v/v) by using a 10^5 (μ-styragel HR5, 30 cm, 15 μm), 10^4, 10^3, 500 Å (PL GEL, 30 cm, 5 μm). The calibration curve was obtained with monodispersed polystyrene standards.
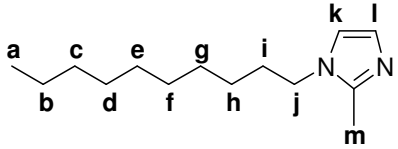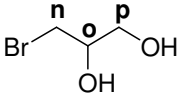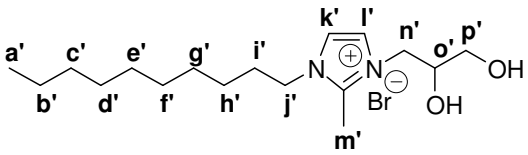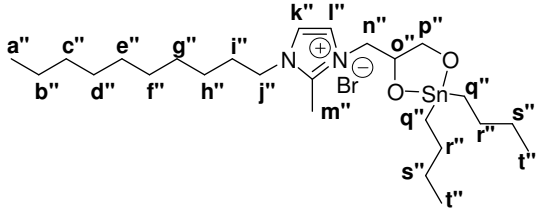
^{1}H NMR spectra were measured for solutions in deuterochloroform.

FTIR spectra of reagents and imidazolium salts were recorded as liquid films between NaCl plates with a Spectrum Two FTIR spectrophotometer (Perkin Elmer).

Imidazolium salts were analyzed by DSC between 25 and 300°C (scanning rate 20°C min^{-1}, under N_2), whereas for **PBT**-based samples the temperature range was generally 0-280°C. Thermal stability of **6** was also tested by keeping the specimens in the DSC pan for 1 h at 160 or 270°C under N_2. As for thermogravimetric analyses, the onset degradation temperature measured at < 1 % weight loss (T_d), the temperature at 20% weight loss (T_{d20}), and the temperature of maximum degradation rate ($T_{d\ max}$) were considered. TGA and derivate thermogravimetry (DTG) curves of the clays were recorded from 50 up to 700°C under N_2 (heating rate 20°C min^{-1}). The organic content in the modified MMTs was determined by the residue obtained at 800°C after O_2 introduction (at 700°C) in the instrument furnace (calculated values are corrected by taking into account the amount of adsorbed H_2O). Thermo-oxidative stability of the composites was tested between 30 and 900°C under oxygen flow

Table 1. Chemical structures, ^{1}H NMR (solutions in CDCl$_3$) and FTIR (liquid films) spectroscopic characterization of reagents **3** and **4** and imidazolium salts **5** and **6**.

3

^{1}H NMR (CDCl$_3$, δ_H, ppm): 0.88 (t, 3H, **a**), 1.28 (m, 14H, **b-h**), 1.71 (q, 2H, **i**), 2.37 (s, 3H, **m**), 3.81 (t, 3H, **j**), 6.81 (d, 1H, **k**), 6.90 (d, 1H, **l**).

FTIR (ν, cm^{-1}): 3390 (N-H stretch), 3106 (=C-H stretch), 2954 (CH$_3$ stretch), 2926 (CH$_2$ stretch), 2855 (CH stretch), 1499 (C-N stretch), 1463 (C-C and CH$_2$ bend), 1424 (H-C-C stretch, H-C-N bend, H-C-C bend), 1276 (imidazolium ring breathing), 1142 (N-H bend), 982 (C-H bend), 722 (CH$_2$ rocking), 676 (imidazolium ring torsion).

4

^{1}H NMR (CDCl$_3$, δ_H, ppm): 2.66 (d, 2H, O**H**), 3.50 (sep, 2H, **n**), 3.74 (qd, 2H, **p**), 3.95 (m, 1H, **o**).

FTIR (ν, cm^{-1}): 3364 (O-H stretch), 2934 (CH$_2$ stretch), 2882 (CH stretch), 1063 and 1030 (C-O stretch), 665 (C-Br stretch).

5

^{1}H NMR (CDCl$_3$, δ_H, ppm): 0.88 (t, 3H, **a'**), 1.28 (m, 14H, **b'-h'**), 1.71 (q, 2H, **i'**), 2.38 (s, 3H, **p**), 3.26 (s, 2H, O**H**), 3.50 (sep, 2H, **n'**), 3.75 (dq, 2H, **p'**), 3.81 (t, 3H, **j'**), 3.95 (m, 1H, **o'**), 6.81 (d, 1H, **k'**), 6.89 (d, 1H, **l'**).

FTIR (ν, cm^{-1}): 3330 (O-H stretch), 3113 (=C-H stretch), 2954 (CH$_3$ stretch), 2926 (CH$_2$ stretch), 2855 (CH stretch), 1501 (C-N stretch), 1463 (C-C and CH$_2$ bend), 1426 (H-C-C stretch, H-C-N bend, H-C-C bend), 1278 (imidazolium ring breathing), 1068 and 1038 (C-O stretch), 982 (C-H bend), 730 (CH$_2$ rocking), 677 (imidazolium ring torsion).

6

^{1}H NMR (CDCl$_3$, δ_H, ppm): 0.92 (m, 9H, **a''** and **t''**), 1.32 (m, 18H, **b''-h''** and **u''-v''**), 1.65 (m, 4H, **i''** and **q''**), 2.36 (d, 5H, **m''** and **n''**), 3.81 (t, 3H, **j''**), 6.81 (d, 1H, **k''**), 6.89 (d, 1H, **l''**), 7.18 (m, 2H, **p''**), 7.26 (m, 1H, **o''**).

FTIR (ν, cm^{-1}): 3026 (=C-H stretch), 2955 (CH$_3$ stretch), 2925 (CH$_2$ stretch), 2855 (CH stretch), 1496 (C-N stretch), 1464 (H-C-C and CH$_2$ bend), 1425 (H-C-C stretch, H-C-N bend, H-C-C bend), 1276 (imidazolium ring breathing), 1079 and 1053 (C-O stretch), 988 (C-H bend), 729 (CH$_2$ rocking), 677 (imidazolium ring torsion), 564 (Sn-C stretch), 456 (Sn-O stretch).

(20°C min^{-1}) and the inorganic content was calculated as residue at the end of the experiment.

Wide angle X-ray diffraction (WAXD) patterns were obtained at 20°C using a Siemens D-500 diffractometer equipped with a Siemens FK 60-10 2000W tube (Cu K$_\alpha$ radiation, λ = 0.154 nm). The operating voltage and current were 40 kV and 40 mA, respectively. Data were collected from 5 to 35 °2θ at 0.02 °2θ intervals.

The morphology of **PBT/6-MMT** composites was investigated by transmission electron microscopy (TEM) using a Zeiss EM 900 microscope operating at an accelerating voltage of 80 kV. Ultra-thin sections (about 50 nm thick) were prepared with a Leica EM FCS cryoultramicrotome equipped with a diamond knife by keeping the sample at -80°C.

Results and discussion

This project involves: (i) the synthesis of a tin-based catalyst **6** incorporating an imidazolium residue; (ii) experiments to establish whether **6** is an effective transesterification catalyst; (iii) immobilization of catalyst **6** by ion exchange with a sodium montmorillonite; (iv) the synthesis of nanocomposites by use of the immobilized catalyst **6**, or a similar catalyst formed *in situ* from **5** and di-*n*-butyldimethoxytin, to polymerize **2** via ED-ROPs; and (v) characterization of the nanocomposites.

Synthesis of tin-based catalyst 6 incorporating an imidazolium salt residue

The synthesis was achieved using the two reactions shown in Scheme 2. First dialkylimidazole **3** was further alkylated with 3-bromo-1,2-propanediol (**4**). The product was then reacted with di-*n*-butyldimethoxytin to form, by a condensation reaction, 1,3-dioxa-2-stannolane **6**. Both reactions were accomplished using reaction conditions similar to those used in analogous reactions described in the literature.[26-31] The product

formation of both reactions was followed by ^{1}H NMR spectroscopy as detailed in ESI. ^{1}H NMR analysis allowed to establish a better reaction time and stoichiometry. Compounds **5** and **6**, both obtained in practically quantitative yield, were characterized by FTIR and ^{1}H NMR spectroscopy (Table 1).

DSC curves (not shown here) of imidazolium salts **5** and **6** exhibit a broad and intense exothermic peak between 110 and 200°C (*ΔH* = -63 J g^{-1}) and between 170 and 290°C (*ΔH* = -300 J g^{-1}), respectively. This phenomenon can be attributed to the thermal degradation of the products, indicating that **6** is more stable than **5**. Stability tests on specimens of **6** were also carried out in the DSC under isothermal conditions at 160°C and at 270°C under N$_2$. No phenomenon was detected during the test conducted at 160°C until more than 50 min; while at 270°C the degradation started after 5 min taking place very rapidly in 6-8 min. These findings were confirmed by TGA analysis under N$_2$ (see Fig. 3) that indicates for product **6** a two-step degradation profile with temperatures of maximum degradation rate (*T$_{d\ max}$*) of 270 and 430°C. The enhanced stability of **6** is very promising. It might be further improved after its intercalation in between the **MMT** layers, as known for ammonium salts.[20]

Performance of 6 for catalyzing ED-ROPs of 2

To assess the performance of **6** as a catalyst for ED-ROPs, MCOs **2** were required. These were prepared by cyclo-depolymerization (CDP) of **PBT** (**1**) as described previously.[12] It was anticipated that the "crude" **BT-MCOs** obtained might contain residues of the di-*n*-butyltin oxide (Bu$_2$SnO) catalyst used for the CDP and that these might be sufficient to catalyze ED-ROP of the MCOs simply by heating without the addition of any catalyst. Elemental analysis for tin indicated that the "crude" **2** contained 0.55% tin.

To carry out a possible ED-ROP, MCOs **2** were heated alone at 190°C for 2 h, the reaction conditions to be used for all the experiments summarized in Table 2.
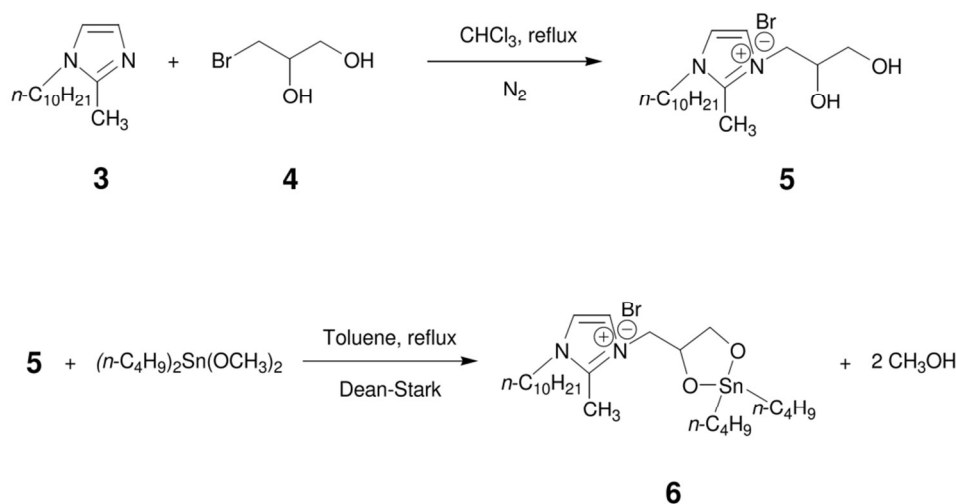
Scheme 2 Synthetic pathways used for the preparation of imidazolium salts **5** and **6**.

.

Table 2. ED-ROP reactions of **2** at 190°C with 1 mol% of catalyst under N_2 for 2 h.[a]

Entry	Catalyst	Total yield[b] (wt%)	Polymer (and MCOs) fraction (%)	$\overline{M_w}$ (10^{-3} g mol^{-1})	$\overline{M_w}/\overline{M_n}$
1[c]	-	60	52 (48)	23.9 (1.8)[d]	1.7
2	-	65	4 (96)	5.6 (1.1)[d]	1.1
3	Bu$_2$Sn(OMe)$_2$	69	65 (35)	41.8 (1.2)[d]	2.6
4	**5**	43	17 (83)	20.0 (1.3)[d]	1.6
5	**5** + Bu$_2$Sn(OMe)$_2$	85	86 (14)	32.0 (1.6)[d]	1.8
6	**6**	89	95 (5)	37.4 (1.3)[d]	2.3

[a] Data obtained by GPC analysis of re-precipitated products. [b] The precipitated polymer plus recovered MCOs. [c] Run carried out on 'crude' **BT-MCOs**. [d] $\overline{M_w}$ of the recovered MCOs fraction.

At the end of the reaction period the reaction mixture was dissolved in dichloromethane/trifluoroacetic acid (80/20 v/v) and precipitated into methanol. The precipitate was collected, dried and analyzed by GPC. This gave **1** in a yield of 52%: see Table 2, entry 1. The polymer had $\overline{M_n}$ 14 100 and $\overline{M_w}$ 23 900 g mol^{-1}. Clearly the 'crude' MCOs **2** were not sufficiently free of catalyst residues. The 'crude' MCOs in chloroform and acetone (94/6 v/v/) were, therefore, passed down a column of activated basic alumina. The 'pure' MCOs obtained were found to contain < 0.10% tin and heating them alone as before gave only a 4% yield of polymer with $\overline{M_n}$ 5 100 and $\overline{M_w}$ 5 600 g mol^{-1}: see Table 2, entry 2. These 'pure' MCOs were used for all subsequent polymerizations. It should be stressed that the intention of the other experiments summarized in Table 2 was not to obtain high yields of polymer but to make comparisons. The catalysts (1 mol%) investigated included di-*n*-butyldimethoxytin (see Table 2, entry 3) and the imidazolium salt **3** (Table 2, entry 4). As expected the former gave a good yield of polymer with good molecular weights, but surprisingly the salt **5** was also a catalyst, albeit a relatively poor one. Use of di-*n*-butyldimethoxytin and **5** together, so that **6** could be formed *in situ*, was more effective (see Table 2, entry 5) than either alone. Finally preformed catalyst **6** was shown to be the most effective catalyst (see Table 2, entry 6) giving a 95% yield of **PBT** (**1**) of $\overline{M_n}$ 16 300 and $\overline{M_w}$ 37 400 g mol^{-1}.

Finally it should be noted that with imidazolium salts **5** and **6**, in each case a small peak was observed in the GPC corresponding to $\overline{M_w}$ of about a million. This is too high for a condensation polymer and suggests that the imidazolium salts were acting as surfactants and that this resulted in some micelle formation.[32]

Modification of montmorillonites

The imidazolium salts **5** and **6** were intercalated between the layers of natural **MMT** by the simple process of ion exchange. In this the sodium cations in the **MMT** galleries are exchanged for imidazolium cations, as detailed in the experimental section. Elemental analyses for nitrogen and tin indicated that **5-MMT** contained 0.68 mmol/g of imidazolium ions whilst **6-MMT** had 0.43 mmol/g of imidazolium ions and 0.20 mmol/g of tin. Thus in the case of **5-MMT** it appears the imidazolium ions

quantitatively exchanged the sodium ions, whereas for **6-MMT** the elemental analysis results, besides indicating a not complete substitution of the alkali cations originally present in the clay galleries, suggest as well a partial ring-opening of the 1,3-dioxa-2-stannolane ring, with loss of the tin-containing moiety. Thermogravimetric studies were performed both on natural clay and the imidazolium-modified clays in order to check their thermal stability and organic content. The results are presented in Table 3 and Fig. 3.
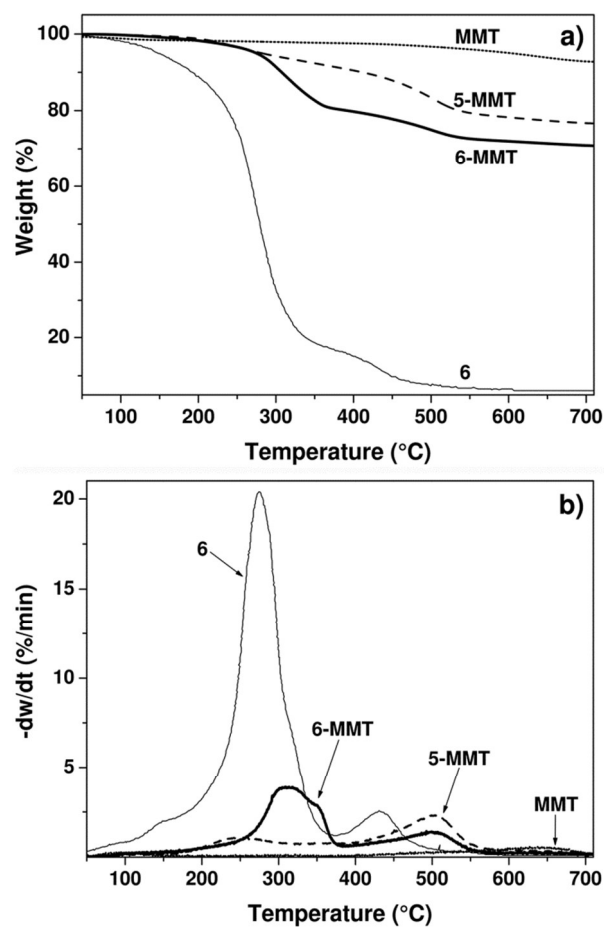

Fig. 3 TGA (a) and DTG (b) curves under N_2 flow of **MMT**, **5-MMT** and **6-MMT**. The curves related to sample **6** are also reported for comparison purpose.

Table 3. Dynamic TGA analysis under N_2 of **MMTs**.

Sample	$T_{d\,max1}$[a] (°C)	$T_{d\,max2}$[b] (°C)	H_2O weight loss @ 150°C (wt%)	Weight loss @ 800°C (wt%)	Inorganic residue @ 800°C (wt%)
MMT	640	-	1	7	92
5-MMT	250	510	< 1	24	76
6-MMT	320	510	1	27	72

[a] Temperature of maximum degradation rate of the first degradation step. [b] Temperature of maximum degradation rate of the second degradation step.

The TGA profile of natural **MMT** exhibits two broad degradation peaks: the first, at about 150°C, corresponds to the loss of adsorbed water and the second, between 400 and 700°C, is due to the dehydroxylation of structural hydroxyl groups of the silicate layers.[20,24] In the case of **5**-**MMT** and **6**-**MMT** samples the loss of adsorbed water is also observed. The decomposition behaviour of **5**-**MMT** and **6**-**MMT** differs significantly from that of pristine **MMT** in the temperature range 200-500°C, that is, in the range in which organic modifiers decompose. Indeed, two distinct decomposition phenomena were observed for the two imidazolium-modified clays: centred at 250 and 510°C for **5**-**MMT** and at 320 and 510°C for **6**-**MMT**. It is worthwhile recalling here that ammonium salts bearing long alkyl chains and intercalated between clay layers are significantly less stable. Indeed, dimethyldialkylammonium **MMT**s exhibit three to four DTG peaks in the range from 200 to 500°C.[20] In particular, for Dellite 67G®, which is a commercial organoclay commonly used for polymer-based composites, the first DTG peak is at about 250°C (data not shown), i.e., 70°C below that of **6**-**MMT**. The inorganic residues measured at 800°C, that is after burning off the organic part of the sample by the introduction of oxygen into the TGA furnace, for the **5**- and **6**-**MMT**s are both around 75 wt%. Taking into account that **5** and **6** have different formula weights and **6** contains a tin atom which remains with the inorganic residue, one can infer that **6** intercalates to a minor extent with respect to **5**. This is in accordance with the above mentioned results of elemental analysis, which indicate contents of nitrogen and tin minor than expected for **6**-**MMT**.

Besides, it is worth noting that the thermal stability of **6** was remarkably enhanced, as desired, after being intercalated in between the clay layers. Indeed, the $T_{d\,max}$ of the first

degradation step ($T_{d\,max1}$) of **6**-**MMT** is 50°C higher than that of neat **6** (see paragraph on Synthesis of **6** and Fig. 3).

A combined TGA-FTIR analysis was carried out on **6**-**MMT** to investigate the volatiles being produced during the two-step degradation process. The results, which evidenced the formation of volatiles due to the degradation of imidazolium modifier, are reported in ESI. The crystalline structures of pristine and imidazolium-modified clays were investigated by WAXD in order to obtain evidence as to whether organic molecules were intercalated between the clay layers. As shown in Fig. 4, the d_{001} layer spacings of the **5**- and **6**-**MMT**s is enlarged compared to that of the natural **MMT**, indicating intercalation of imidazolium salts between clay layers. In the particular case of **6**-**MMT**, a reflection at a 2θ value corresponding to that of the pristine clay is also present, confirming the incomplete ion-exchange reaction during clay modification, probably due to the modest solubility of **6** in the acetonitrile medium.

Synthesis of nanocomposites

Nanocomposites were prepared by carrying out ED-ROPs of **BT-MCOs** in the presence of 3 wt% of natural or imidazolium-modified **MMT**. The **BT-MCOs** were previously intercalated in between the clay layers, as detailed in the Experimental section. As summarized in Table 4, the reactions were carried out at 190°C for 2 h in the presence or not of the various catalytic systems described above. Similarly to what found for ED-ROP reactions carried out in the absence of clay (see Table 2), the fractions with $\overline{M_w} < 2\,000$ were ascribed to recovered MCOs.

As expected, in the absence of a transesterification catalyst (Table 4, entry 1) or in the presence of **5**-**MMT** (Table 4, entry 3), ED-ROP does not occur at all as it is evident from the complete recovery of unreacted MCOs.

Table 4. **PBT**-based nanocomposites by ED-ROP of purified **BT-MCOs** at 190°C with 1 mol% of catalyst under N_2 for 2 h.[a]

Entry	Sample composition	Total yield[b] (wt%)	Polymer (and MCOs) fraction (%)	$\overline{M_w}$ (10^{-3} g mol^{-1})	$\overline{M_w}/\overline{M_n}$
1	**MMT**	55	- (100)	- (1.1)[c]	-
2	**MMT** + Bu$_2$Sn(OMe)$_2$	91	91 (9)	29.2 (1.5)[c]	2.3
3	**5-MMT**	45	- (100)	- (1.1)[c]	-
4	**5-MMT** + Bu$_2$Sn(OMe)$_2$	91	95 (5)	37.4 (1.5)[c]	2.4
5	**6-MMT**	94	96 (4)	50.4 (1.5)[c]	2.0

[a] Data obtained by GPC analysis of re-precipitated products. [b] The reprecipitated polymer plus recovered MCOs. [c] $\overline{M_w}$ of the recovered MCOs fraction

.

The presence of Bu$_2$Sn(OMe)$_2$ (Table 4, entries 2 and 4) promotes increases of both the polymer yield and its $\overline{M_w}$. This effect is even greater when this catalyst is used in combination with **5**-**MMT** (Table 4, entry 4) with respect to pristine **MMT** (Table 4, entry 2).

Comparing entry 4 of Table 2 with entry 3 of Table 4, suggests that the low catalytic activity of **5** is further reduced after supporting it on **MMT**. Only after the addition of Bu$_2$Sn(OMe)$_2$ to **5-MMT** (Table 4, entry 4) were better results obtained.

As desired, and in part expected on the basis of results previously obtained by using the imidazolium salt **6** as a catalyst for the ED-ROP reaction of **2**, the use of **6-MMT** as a supported catalytic system (Table 4, entry 5) resulted in the highest polymer fraction yield (> 95%) and in the highest $\overline{M_w}$ (50 400 g mol^{-1}). Moreover, the $\overline{M_w}$ is even higher than that obtained in the analogous reaction performed in the absence of **MMT** (Table 2, entry 6). A synergistic catalytic effect between **MMT** and the transesterification catalysts Bu$_2$Sn(OMe)$_2$ and **6** can be inferred.

Following the success of the experiment summarized in Table 4, entry 5, the experiment was repeated on a larger scale but using mechanical stirring. The polymerization is very fast and within 3 min the molten reaction mixture became too viscous to

be mechanically stirred. The reaction was continued for a total time of 30 min. Differently from the other reactions, the ensuing product was almost insoluble in a mixture of dichloromethane-trifluoroacetic acid (80/20 v/v). The yield was practically quantitative (97 wt%) and the level of unreacted **BT-MCOs** below 2 wt% (from GPC). The **PBT** polymer had $\overline{M_w}$ 80 000 g mol^{-1} and $\overline{M_w}$/$\overline{M_n}$ = 2.0. These values are comparable to those of the commercial **PBT** used here: $\overline{M_w}$ 85 500 g mol^{-1}; $\overline{M_w}$/$\overline{M_n}$ = 1.8.

Characterization of the nanocomposites

The nanocomposite samples were carefully characterized using various techniques.

The following discussion on XRD and TEM characterizations refers in particular to the **PBT/6-MMT** nanocomposite prepared by *in situ* ED-ROP of **2** using mechanical stirring. In Fig. 5, X-ray diffraction patterns of the **2/6-MMT** (97/3) mixture recorded before (trace c) and after (trace d) ED-ROP reaction of the macrocycles are compared. WAXD patterns of neat **BT-MCOs** (**2**) (trace b) and commercial **PBT** polymer (trace a) are also reported for comparison, and the position of reflections characteristic of **6-MMT** are marked.
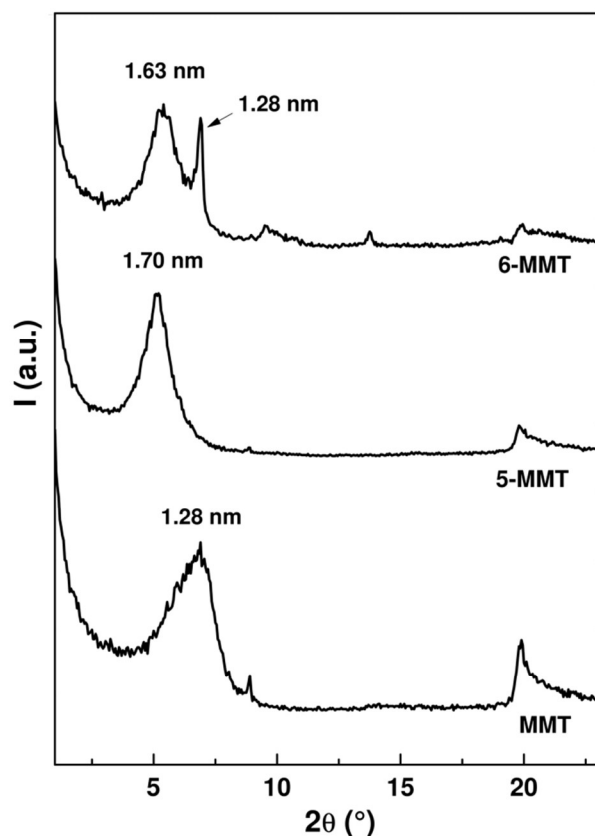

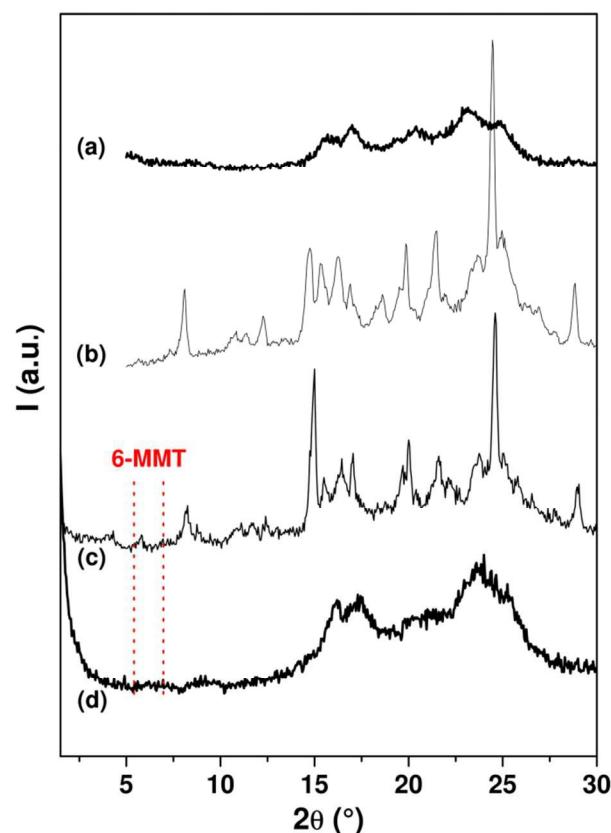**Fig. 4** WAXD profiles of pristine **MMT** and imidazolium-modified **5-MMT** and **6-MMT**.

Fig. 5 X-ray diffraction patterns of: (a) **PBT**; (b) **BT-MCOs** (**2**); and **BT-MCOs/6-MMT** 97/3 mixture recorded before (c) and (d) after ED-ROP reaction. The positions of reflections characteristic of the **6-MMT** clay are also shown.

RSC Advances

ARTICLE

Journal Name

Before the ED-ROP reaction, in the diffraction pattern of the **2/6-MMT** mixture (trace c), at high 2θ values (namely, between 7 and 30° 2θ) the sharp and strong reflections characteristic of **BT-MCOs** (trace b) are found. After the polymerization reaction took place the diffraction pattern of the ensuing composite (trace d) become quite similar (as expected) to that of the commercial sample of **PBT** (trace a). These findings clearly confirm the occurrence of MCOs polymerization by ED-ROP. Moreover, in the **2/6-MMT** (97/3) mixture (trace c) the reflections corresponding to the d_{001} of the **6-MMT** are remarkably reduced in intensity, due to the low amount of clay stacks, and shifted towards lower values of 2θ, indicating the effective intercalation of macrocycles **2** in between the layers of the imidazolium-modified clay which maintains a certain crystalline order. After the polymerization reaction takes place, no peak attributable to the clay is practically detectable (trace d), suggesting a high disruption of the clay order.

The dispersion of clay layers in the **PBT/6-MMT** nanocomposite obtained from *in situ* ED-ROP was investigated by TEM observation carried out at different magnifications and in several zones of the sample. Some representative TEM micrographs are shown in Fig. 6. Very few clay aggregates with diameters below 1-2 μm, together with sub-micrometric stacks and tactoids containing a few layers, quite homogeneously distributed, are observable within the **PBT** matrix (Fig. 6a,b). The presence of many isolated clay layers and stacks containing highly disordered layers (Fig. 6c,d) confirms the high extent of **MMT** delamination suggested by WAXD analysis. A quite similar clay dispersion (images not shown) was observed also in the corresponding **PBT/6-MMT** nanocomposite obtained from *in situ* ED-ROP of **2** without mechanical stirring (Table 4, entry 5), confirming the working hypothesis that the imidazolium salt enters the gap between clay layers and ED-ROP reaction occurs in between the layers.

DSC analysis was carried out on the nanocomposites in order to evidence differences in the thermal behaviour: no relevant nucleation effect promoted by the clay on the crystallization of the **PBT** matrix was indeed observed.
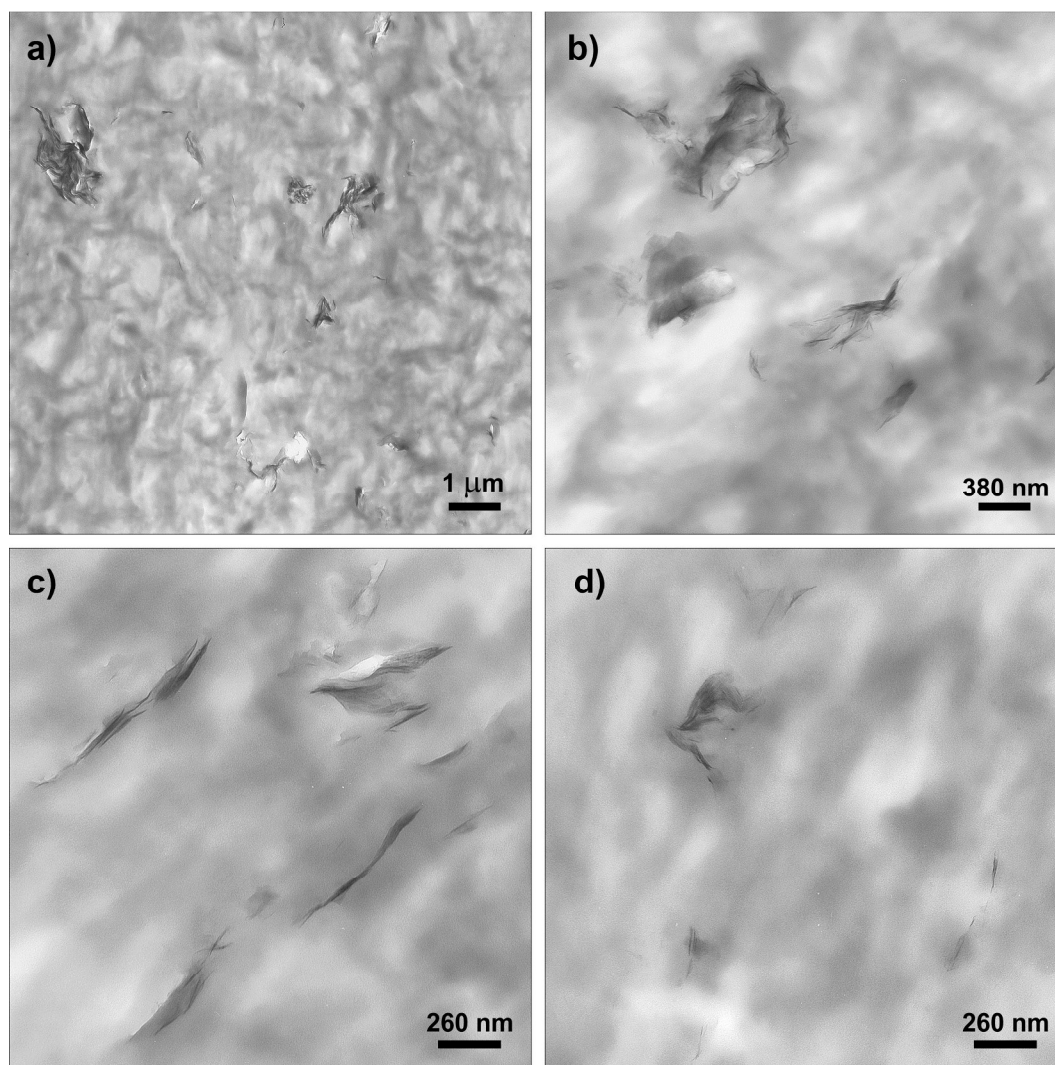

Fig. 6. TEM micrographs at different magnifications of the **PBT/6-MMT** nanocomposite obtained from *in situ* ED-ROP of **2**.

RSC Advances Accepted Manuscript

Dynamic TGA experiments indicate that, with respect to a **PBT** sample obtained by ED-ROP of **BT-MCO**s (Table 2, entry 2), thermo-oxidative stability of the **PBT**-based nanocomposites is higher of about 10°C for T_d and 20°C for $T_{d\,max}$.

Conclusions

The novel robust functionalized imidazolium salt **6**, bearing a 1,3-dioxa-2-stannolane moiety capable of catalyzing transesterification reactions, was successfully synthesized and thoroughly characterized.

The efficacy of the functionalized imidazolium salt as a transesterification catalyst was proven in the ED-ROP reaction of macrocyclic oligomers of **PBT** (**BT-MCO**s). The functionalized imidazolium salt was inserted between the montmorillonite (**MMT**) clay layers by ion exchange.

PBT-based nanocomposites containing the imidazolium-modified **MMT** were successfully prepared through *in situ* ED-ROP reaction of **BT-MCO**s previously intercalated in between the clay layers.

BT-MCOs conversion, **PBT** molecular weights, thermo-oxidative stability and final morphology of the nanocomposites were improved by the positive synergistic effect exerted by the transesterification catalyst moiety borne by the imidazolium salt intercalated in between the **MMT** layers.

Acknowledgements

Notes and references

[a] Istituto per lo Studio delle Macromolecole (ISMAC) – UOS Genova, Consiglio Nazionale delle Ricerche (CNR), Via De Marini 6, Genova, 16149, Italy. E-mail: conzatti@ge.ismac.cnr.it; Tel: +39-010-6475866; Fax: +39-010-6475880.

[b] Department of Chemistry, University of Manchester, Oxford Road, Manchester, M13 9PL, UK.

† Electronic Supplementary Information (ESI) available: [details of any supplementary information available should be included here]. See DOI: 10.1039/b000000x/

1   M. Alexandre, P. Dubois, *Mater. Sci. Eng.*, 2000, **28**, 1.

2   S. S. Ray, M. Okamoto, *Prog. Polym. Sci.*, 2003, **28**, 1539.

3   C. H. Davis, L. J. Mathias, J. W. Gilman, D. A. Schiraldi, J. R. Shields, P. Trulove, T. E. Sutto, H. C. Delong, *J. Polym. Sci. Part B: Polym. Phys.*, 2002, **40**, 2661.

4   G. Engelmann, E. Bonatz, J. Ganster, *J. Appl. Polym. Sci.*, 2013, **127**, 3848.

5   C. F. Ou, *J. Polym. Sci. Part B: Polym. Phys.*, 2003, **41**, 2902.

6   T. Y. Tsai, C. H. Li, C. H. Chang, W. H. Cheng, C. L. Hwang, R. J. Wu, *Adv. Mater.*, 2005, **7**, 1769.

7   Y. Imai, S. Nishimura, E. Abe, H. Tateyama, A. Abiko, A. Yamaguchi, T. Aoyama, H. Taguchi, *Chem. Mater.*, 2002, **4**, 477.

8   D. J. Brunelle, *J. Polym. Sci. Part A: Polym. Chem.*, 2008, **46**, 1151.

9   S. Strandman, J. E. Gautrot, X. X. Zhu, *Polym. Chem.*, 2011, **2**, 791.

10   P. Hodge, *Chem. Rev.*, 2014, **114**, 2278.

11   S. D. Kamau, P. Hodge, R. T. Williams, P. Stagnaro, L. Conzatti, *J. Comb. Chem.*, 2008, **10**, 644.

12   M. Alessi, L. Conzatti, P. Hodge, S. Taglialatela Scafati, P. Stagnaro, *Macromol. Mater. Eng.*, 2010, **295**, 374.

13   L. Conzatti, M. Alessi, P. Stagnaro, P. Hodge, *J. Polym. Sci. Part A: Polym. Chem.*, 2011, **49**, *995.*

14   A. R. Tripathy, E. Burgaz, S. N. Kukureka, W. J. MacKnight, *Macromolecules*, 2003, **36**, 8593.

15   C. Berti, E. Binassi, M. Colonna, M. Fiorini, T. Zuccheri, S. Karanam, D. J. Brunelle, *J. Appl. Polym. Sci.*, 2009, **114**, 3211.

16   F. Wu, G. Yang, *Mater. Lett.*, 2009, **63**, 1686.

17   S. C. Hong, S. S. Lee, *Comp. Sci. Technol.*, 2013, **86**, 170.

18   G. Balogh, S. Hajba, J. Karger-Kocsis, T. Czigany, *J. Mater Sci.*, 2013, **48**, 2530.

19   H. Chen, C. Huang, W. Yu, C. Zhou, *Polymer*, 2013, **54**, 1603.

20   W. Xie, Z. Gao, W.P. Pan, D. Hunter, A. Singh, R. Vaia, *Chem. Mater.*, 2001, **13**, 2979.

21   K. Stoeffler, P. G. Lafleur, J. Denault, *Polym. Deg. Stab.*, 2008, **93**, 1332.

22   W. Abdallah, U. Yilmazer, *Thermochim. Acta*, 2011, **525**, 129.

23   V. Mittal, *Appl. Clay Sci.*, 2012, **56**, 103.

24   W.H. Awad, J.W. Gilman, M. Nyden, R. H. Harris, T. E. Sutto, J. Callahan, P. C. Trulove, H. C. Delong, D. M. Fox, *Themochim. Acta*, 2004, **409**, 3.

25   P. Hodge, *React. Funct. Polym.*, 2014, **80**, 21.

26   J. Langat, S. Bellayer, P. Hudrlik, P. H. Maupin, J. W. Gilman, D. Raghavan, *Polymer*, 2006, **47**, 6698.

27   E. Tarkin-Tas, S. K. Goswami, B. R. Nayak, L. J. Mathias, *J. Appl. Polym. Sci.*, 2008, **107**, 976.

28   H. R. Kricheldorf, S. R. Lee, N. Schittenhelm, *Macromol. Chem. Phys.*, 1998, **199**, 273.

29   H. R. Kricheldorf, *J. Polym. Sci. Part A: Polym. Chem.*, 2004, **42**, 4723.

30   G. Reginato, A. Ricci, S. Roelens, S. Scapecchi, *J. Org. Chem.*, 1990, **55**, 5132.

31   H. C. Aspinall, N. Greeves, E. G. McIver, *Tetrahedron*, 2003, **59**, 10453.

32   T. Biedron, M. Brzezinski, T. Biela, P. Kubisa, *J. Pol. Sci. Part A: Pol. Chem.*, 2012, **50**, 4538.

RSC Advances Accepted Manuscript